accepted for publication in Eur. Phys. J. B, (2002)

The European Physical Journal B

Persistence distributions in a conserved lattice gas with absorbing states

S. Lübeck and A. Misra

Theoretische Tieftemperaturphysik, Gerhard-Mercator-Universität Duisburg,
Lotharstr. 1, 47048 Duisburg, Germany

received 27 August 2001

Abstract. Extensive simulations are performed to study the persistence behavior of a conserved lattice gas model exhibiting an absorbing phase transition from an active phase into an inactive phase. Both the global and the local persistence exponents are determined in two and higher dimensions. The local persistence exponent obeys a scaling relation involving the order parameter exponent of the absorbing phase transition. Furthermore we observe that the global persistence exponent exceeds its local counterpart in all dimensions in contrast to the known persistence behavior in reversible phase transitions.

PACS. 0 5.70.Ln, 05.50.+q, 05.65.+b

1 Introduction

In the last decade numerous articles have been devoted to the study of persistence behavior in nonequilibrium systems [1,2,3,4,5,6,7,8,9,10,11]. The basic quantity of interest is the persistence distribution $P(t)$, defined as the probability that a certain physical quantity does not change its state up to time t during a stochastic evolution. The persistence distribution has been observed to decay as $P(t) \sim t^{-\theta}$, where θ is denoted as the persistence exponent. Since the persistence behavior depends on the entire history of evolution of the nonequilibrium process, there are only few instances of an exact calculation of the persistence exponent in the literature [2,7,8]. In general the persistence exponent is nontrivial in the sense that it cannot be obtained from scaling relations, except of certain Markovian systems [4]. There exists two different types of persistence exponent $\theta_{\rm l}$ and $\theta_{\rm g}$ associated with the persistence behavior of the local and the global order parameter, respectively. These two exponents have been observed in general to be different from each other. Usually for reversible phase transitions the inequality $\theta_{\rm g} < \theta_{\rm l}$ is observed, however in the case of the continuous absorbing phase transition of the Ziff-Gulari-Barshad model [12], which belongs to the universality class of directed percolation, the reverse inequality has been observed numerically [11].

Recently Rossi *et al.* introduced a conserved lattice gas (CLG) model that exhibits a continuous phase transition to an absorbing state at a critical value of the particle density [13]. Numerical simulations in various dimensions [14] confirm the conjecture of [13] that the CLG model belongs to a new universality class different from the well known universality class of directed percolation (see [15] for an overview). In this work we consider the persistence distributions of the CLG model in various dimensions ($D = 2, 3, 4, 5$). We determine numerically the global and local persistence exponents as well as the exponent $\nu_\parallel$ which describes the divergence of the correlation time at the transition point. To our knowledge this is the first time that the persistence behavior of a nonequilibrium critical system with absorbing states is investigated in higher dimensions, i.e., below and above the upper critical dimension $D_{\rm c}$. Similar to [11] we observe the reverse inequality $\theta_{\rm g} > \theta_{\rm l}$ for the CLG model. We believe that systems exhibiting irreversible phase transitions into an absorbing state are generally characterized by this reversed inequality in contrast to systems exhibiting a reversible phase transition, in particular equilibrium phase transitions.

The paper is organized as follows. In the next section we describe the CLG model. In section 3 we define the local and the global persistence distributions for this model and describe their steady state scaling behavior in the critical regime. In the following two sections we present the determination of the global (sec. 4) and local (sec. 5) persistence exponents. With a short discussion we conclude the paper in section 6.

2 The CLG model

We consider the CLG model (see [13]) on D-dimensional cubic lattices of linear size L. Initially one distributes randomly $N = \rho L$ particles on the system where ρ denotes

the particle density. In order to mimic a repulsive interaction a given particle is considered as *active* if at least one of its $2D$ neighboring sites on the cubic lattice is occupied by another particle. If all neighboring sites are empty the particle remains *inactive*. Active particles are moved in the next update step to one of their empty nearest neighbor sites, selected at random. Starting from a random distribution of particles the system reaches after a transient regime a steady state which is characterized by the density of active sites $\rho_{\rm a}$. The average density $\langle\rho_{\rm a}\rangle$ is the order parameter of the absorbing phase transition, i.e., it vanishes if the control parameter ρ is lower than the critical value $\rho_{\rm c}$. Approaching the critical value from above the order parameter scales as $\langle\rho_{\rm a}\rangle \sim \delta\rho^{\beta}$, where $\delta\rho = \rho - \rho_{\rm c}$. The order parameter exponent β as well as the scaling behavior of the order parameter fluctuations are investigated numerically in various dimensions in [14]. In our simulations, a random sequential update scheme is applied, i.e., all active sites are updated at each time step in a randomly chosen sequence. The considered system sizes are $L \leq 1024$ for $D = 2$, $L \leq 128$ ($D = 3$), $L \leq 32$ ($D = 4$) and $L \leq 16$ in the case of $D = 5$. All measurements are performed in the steady state and the used equilibration procedures are discussed in detail in [14].

3 Persistence distributions

In this work we consider the persistence behavior of the CLG model. Usually one distinguishes the so-called global persistence distribution $P_{\rm g}(t)$ and the local persistence distributions $P_{\rm l}(t)$. The global persistence characterizes the time evolution of the order parameter, i.e., it characterizes how long the whole system remains in a given phase. For instance in magnetic systems $P_{\rm g}(t)$ can be defined as the probability that the magnetization changes sign after the duration t. At criticality $P_{\rm g}(t)$ is expected (see for instance [6]) to decay algebraically

$$P_{\rm g}(t) \;\sim\; t^{-\theta_{\rm g}}, \tag{1}$$

where the time t corresponds to the number of update steps. Off criticality, the finite correlation time $\xi_{\parallel}$ limits this power-law behavior and the corresponding probability distribution displays a cut-off at $t = \mathcal{O}(\xi_{\parallel})$. Using $\xi_{\parallel} \sim \delta\rho^{-\nu_{\parallel}}$ and standard scaling arguments one expects that the persistence probability obeys the ansatz

$$P_{\rm g}(t) \;=\; \delta\rho^{\nu_{\parallel}\theta_{\rm g}}\, \mathcal{P}_{\rm g}(\delta\rho^{\nu_{\parallel}}\, t), \tag{2}$$

with the universal function $\mathcal{P}_{\rm g}$. Thus the scaling behavior of the probability distribution $P_{\rm g}(t)$ allows to determine beside the persistence exponent $\theta_{\rm g}$ the exponent $\nu_{\parallel}$ of the temporal correlations in all considered dimensions.

The phase transition of the CLG model is an irreversible transition into an absorbing state, i.e., the order parameter $\langle\rho_{\rm a}\rangle$ is a strictly positive quantity. In this cases it is usual [10,11] to measure the probability that the deviation of the density of active sites from the order parameter, i.e. $\rho_{\rm a} - \langle\rho_{\rm a}\rangle$, changes sign after t update steps. Furthermore, the distribution of the deviations could be different below and above $\langle\rho_{\rm a}\rangle$. In order to take this asymmetry into account we calculate two different quantities $P_{\rm g}^{>}(t)$ and $P_{\rm g}^{<}(t)$ corresponding to the global persistence distribution for $\rho_{\rm a}(t) > \langle\rho_{\rm a}\rangle$ and $\rho_{\rm a}(t) < \langle\rho_{\rm a}\rangle$, respectively.

The so-called local persistence is defined as the probability that the local order parameter at a given site, for instance a single spin, remains in a phase, i.e., it does not flip within a duration t. In the case of the CLG model we consider the steady state probability distribution $P_{\rm l}(t)$ that a particle remains inactive for exactly t update steps. Since no spontaneous generation of active sites is allowed in the CLG model, a given site may remain inactive for a long time until it is re-activated in the presence of another active site. Thus one expects that the corresponding probability distribution decays algebraically with an exponent $\theta_{\rm l}$,

$$P_{\rm l}(t) \;\sim\; t^{-\theta_{\rm l}}. \tag{3}$$

Alternatively one may ask how long a given particle remains active. But active sites can be spontaneously "annihilated" to become inactive and the corresponding probability distribution decays exponentially. This "asymmetry" [16] in the dynamical behavior of active and inactive sites is already known from other systems exhibiting an absorbing phase transition, for instance directed percolation.

Above the transition point ($\rho > \rho_{\rm c}$) the local persistence distribution displays a cut-off at $t = \mathcal{O}(\xi_{\rm l})$, where $\xi_{\rm l}$ denotes the correlation time of the effective single site process. Assuming that $\xi_{\rm l}$ scales as $\xi_{\rm l} \sim \delta\rho^{-\nu_{\rm l}}$ one obtains the scaling behavior of the local persistence distribution

$$P_{\rm l}(t) \;=\; \delta\rho^{\nu_{\rm l}\theta_{\rm l}}\, \mathcal{P}_{\rm l}(\delta\rho^{\nu_{\rm l}}\, t) \tag{4}$$

with the local critical exponents $\theta_{\rm l}$ and $\nu_{\rm l}$. These local exponents are connected to the order parameter exponent β. Using the scaling ansatz Eq. (4) one can calculate the average time between two activation events

$$\langle t\rangle \;=\; \int t\, P_{\rm l}(t)\, {\rm d}t \;\sim\; \delta\rho^{-\nu_{\rm l}(2-\theta_{\rm l})}. \tag{5}$$

Approaching the transition point ($\delta\rho \to 0$) the average time between two activation events diverges (we will see that $\theta_{\rm l} < 2$ in all dimensions). The number of activation events within a certain duration is proportional to $1/\langle t\rangle$. On the other hand the number of activations is proportional to the probability that a site is active at a given time. Therefore $1/\langle t\rangle \propto \langle\rho_{\rm a}\rangle$ and this leads to the scaling relation

$$\nu_{\rm l}\,(2 - \theta_{\rm l}) \;=\; \beta. \tag{6}$$

In spatially extended systems the time evolution of a single site is coupled to that of its neighbors, thus the effective single site evolution is non-Markovian. In this sense the local persistence distribution is related to an infinite point correlation function (see for instance [11,16]) whereas the persistence distribution of the order parameter is related to a two-point correlation function. Thus one expects that the exponent $\nu_{\rm l}$ does not agree with the

exponent of the order parameter $\nu_\perp \neq \nu_\parallel$. But this inequality does not imply that the order parameter scaling behavior of the CLG model is characterized by an additional second correlation time because $\nu_\perp$ just describes the temporal correlations of an effective single site time-series and not of the temporal evolution of the order parameter. Furthermore, one may expect for the same reason that the persistence exponents are different, i.e., $\theta_g \neq \theta_\perp$. Previous investigations suggest a general behavior with $\theta_g < \theta_\perp$. In this case the persistence behavior of the global properties are stronger than those of the local properties. For instance the average duration between two spin flips in ferromagnetic systems is smaller than the duration between order parameter flips. Recently, a violation of this inequality was reported by Hinrichsen and Kodu-vely who observed $\theta_g \approx \theta_\perp$ in the case of directed percolation [16]. Additionally the persistence distributions of the Ziff-Gulari-Barshad model [12], which exhibits a continuous absorbing phase transition belonging to the directed percolation universality class, are characterized in the "long-time regime" [11] by the inequality $\theta_g > \theta_\perp$ for $D = 2$.

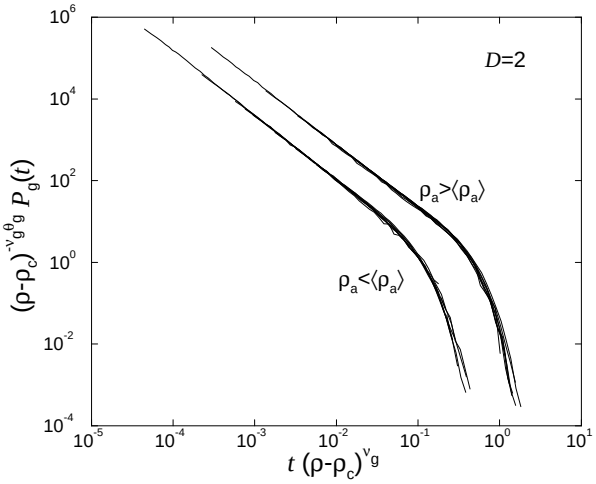

Fig. 2. Scaling analysis of the two-dimensional global persistence distributions $P_g^<(t)$ and $P_g^>(t)$. In the case of $P_g^<(t)$ the curves are shifted in the lower-left direction. The values of the exponents are presented in the text.

4 Global persistence distributions

We consider the global persistence distributions for dimensions $D = 2, 3, 4$. As explained above one expects a cut-off of the probability distributions for $t \approx \mathcal{O}(\xi_\parallel)$. Thus, $\mathcal{O}(\xi_\parallel)$ update steps have to be performed to measure one of these long-time events. This shows that extensive simulations are required to obtain the global probability distribution with a sufficient accuracy. For instance 5×10^6 single update steps were used in [14] to determine the critical behavior of the order parameter $\langle \rho_a \rangle$ for $D = 2$. Here, we used for similar system parameters 4×10^7 update steps in the steady state which yield approximately 6×10^5 single events for the measurement of the global probability distribution.

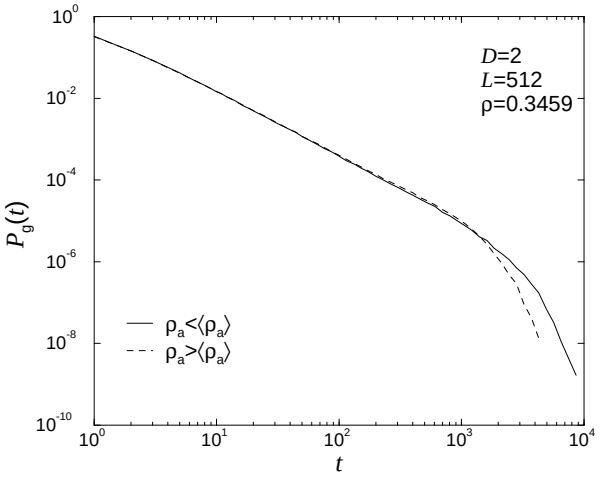

Fig. 1. The global persistence distributions $P_g^<(t)$ and $P_g^>(t)$ for a given system size and particle density. The different asymmetric behavior below and above the average value $\langle \rho_a \rangle$ (see text) can be clearly seen in the cut-off behavior.

Fig. 1 shows the distributions $P_g^>(t)$ and $P_g^<(t)$ for the two-dimensional model in a log-log plot. As one can see the slopes of the curves are nearly the same but the cuf-off behavior differs significantly. Simulations for different values of $\delta\rho$ are performed and the obtained curves are analyzed according to the scaling ansatz Eq. (2). In the case of the two-dimensional model we obtain a good data collapse for $\theta_g^> = 1.57 \pm 0.05$, $\nu_\parallel^> = 1.15 \pm 0.04$ and $\theta_g^< = 1.60 \pm 0.06$, $\nu_\parallel^< = 1.18 \pm 0.05$, respectively. The corresponding curves are shown in Fig. 2. Although the distributions $P_g^>(t)$ and $P_g^<(t)$ differ at the cut-offs the scaling behavior, i.e. the exponents, of both distributions agree within the error-bars.

Our simulations yield that the different cut-off behavior of $P_g^>(t)$ and $P_g^<(t)$ vanishes with increasing dimension. Therefore, no significant differences between the exponents $\theta_g^{>,<}$ and $\nu_\parallel^{>,<}$ are observed in higher dimensions too. In the case of the three dimensional model sufficient data collapses (see Fig. 3) are obtained for the values $\theta_g^> = 1.53 \pm 0.06$, $\nu_\parallel^> = 1.03 \pm 0.03$ and $\theta_g^< = 1.54 \pm 0.06$, $\nu_\parallel^< = 1.05 \pm 0.03$.

It is known that that the upper critical dimension of the CLG is $D_c = 4$ [14]. Thus one expects that a data-collapse of the corresponding curves is obtained if one uses the mean-field values of the exponent, i.e., $\nu_\parallel = 1$ and $\theta_g = 3/2$. In the latter case we assume that the time series of the order parameter can be mapped to a generalized random walk. Using these values a good data-collapse is obtained which is plotted in Fig. 3.

5 Local persistence distributions

We consider the local persistence distribution $P_{\rm l}(t)$ of the CLG model for $D = 2, 3, 4, 5$. Compared to the global persistence fewer update steps are needed to determine the local persistence distribution for a similar degree of accuracy because the time evolution of all particles ($N = L^D\rho$) can be used to measure $P_{\rm l}(t)$. Similar to the above analysis one varies again the exponents $\theta_{\rm l}$ and $\nu_{\rm l}$ until one gets a data-collapse of different curves which correspond to different values of $\delta\rho$. The resulting data-collapses for $D = 2, 3, 4, 5$ are plotted in Fig. 4. The local persistence exponent decreases from $\theta_{\rm l} = 1.41 \pm 0.02$ for $D = 2$ to $\theta_{\rm l} = 1.19 \pm 0.03$ for $D = 3$. For $D \geq 4$ good data-collapses are obtained for $\theta_{\rm l} = 1$, i.e., our results suggest that the mean-field value is $\theta_{\rm l} = 1$.

The values of the local correlation exponent $\nu_{\rm l}$ decreases from $\nu_{\rm l} = 1.10 \pm 0.02$ ($D = 2$) to $\nu_{\rm l} = 1.04 \pm 0.03$ ($D = 3$). In the case of $D = 4$ we used $\nu_{\rm l} = 1$ to obtain the data-collapse. Surprisingly a significantly different value $\nu_{\rm l} = 1.08 \pm 0.03$ has to be used to produce a data-collapse for $D = 5$ (see Fig. 4). But in the case of the five-dimensional system the simulations are limited by the available system sizes ($L \leq 16$). Therefore, it is possible that the above value describes a certain transient regime instead of the real critical scaling behavior. Therefore, we think that $\nu_{\rm l} = 1$ describes the actual mean-field behavior.

In the following we check the scaling relation Eq. (6) which connects the exponents β, $\nu_{\rm l}$ and $\theta_{\rm l}$ in the steady state. For $D = 2$ our numerically obtained result $\nu_{\rm l}(2 - \theta_{\rm l}) = 0.649$ agrees with the result $\beta = 0.637 \pm 0.009$ from [14]. In the case of $D = 3$ we get $\nu_{\rm l}(2 - \theta_{\rm l}) = 0.842$ which agrees again with $\beta = 0.837 \pm 0.015$ obtained from the same reference. Finally the values $\nu_{\rm l} = 1$, $\theta_{\rm l} = 1$, and $\beta = 1$ [14,17] fulfill the scaling relation exactly which confirms the above conclusion that $\nu_{\rm l} = 1$ is valid for $D \geq 4$.

It is worth considering the average number of activations within a certain time ($n_{\rm act} \sim 1/\langle t\rangle$) in detail. Using the Eqs. (5,6) one sees that $n_{\rm act}$ decreases with the dimension, i.e., $n_{\rm act}^{(D)} > n_{\rm act}^{(D+1)}$ for $\delta\rho \to 0$ because $\beta^{(D)} < \beta^{(D+1)}$. This suggests that the probability to re-activate a given site decreases with increasing dimension. This result could be surprising at first sight since one would expect that due to the increasing number of next neighbors in higher dimensions it is more likely to re-activate a given lattice site. But the increasing number of next neighbors results in a reduced re-activation probability. We guess that this behavior is caused by a reduced return probability of activations, similar to a random walk. The probability that a symmetric random walk ever returns to its origin is certain for $D = 1$ and $D = 2$ but uncertain for $D = 3$ (see for instance [18]). In the case of the CLG model one can assume that close to criticality only few activations diffuse through the system. Increasing the dimension it becomes less likely that these activations return to their origins.

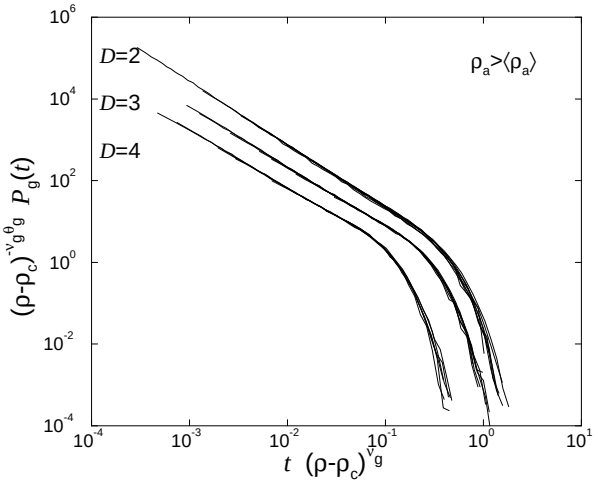

Fig. 3. Scaling analysis of the global persistence distribution $P_{\rm g}^{>}(t)$ for various dimensions. With increasing dimensions the slope of the curves (i.e. the exponent $\theta_{\rm g}$) decreases slightly. The curves of the three- and four-dimensional system are shifted in the lower-left direction. The corresponding data-collapses for $P_{\rm g}^{<}(t)$ are of similar accuracy (not shown).

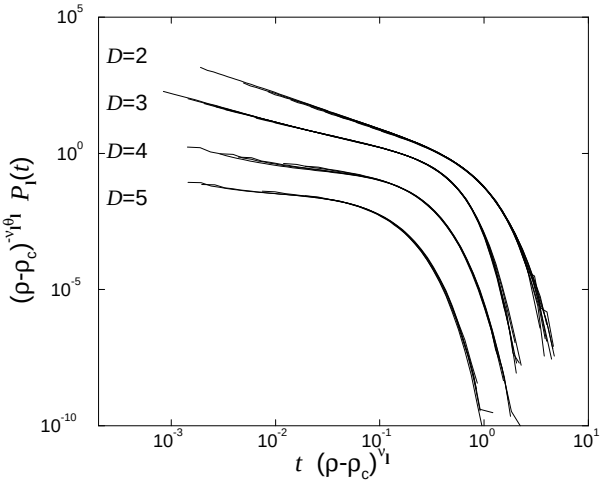

Fig. 4. Scaling analysis of the local persistence distribution $P_{\rm l}(t)$ for various dimensions. With increasing dimensions the slope of the curves (i.e. the exponent $\theta_{\rm l}$) decreases. For $D = 3, 4, 5$ the corresponding curves are shifted in the lower-left direction.

6 Discussion

Considering the results of the local and global persistence exponents (see Table 1) one concludes that the CLG model is characterized by the reversed persistence behavior $\theta_{\rm g} > \theta_{\rm l}$. The usual behavior $\theta_{\rm g} < \theta_{\rm l}$ was observed in reversible equilibrium phase transitions and means that the global order parameter persists longer in a given phase than the corresponding local quantities. For instance it is more

likely in a magnetic system that a single spin flips than the magnetization.

Our result and the similar one of [11] suggest that critical systems with absorbing states behaves generally different from reversible equilibrium systems. Here, the order parameter fluctuates on smaller scales than the local sites. Approaching the transition point ($\delta\rho \to 0$) only a few sites are activated. Considering snapshots of the CLG model we observed that these activated sites are concentrated around small regions of activation which "diffuses" very slowly through the system. Thus non-active particles persist for a long time in their state until they are reactivated by other active particles. But the order parameter fluctuates around its mean value within this time. This behavior is a common feature of absorbing phase transitions and we therefore think that systems exhibiting an absorbing phase transitions are generally characterized by the reversed persistence behavior $\theta_{\rm g} > \theta_{\rm l}$.

Table 1. The critical exponents of the CLG model for various dimensions D. The symbol * denotes logarithmic corrections to the power-law behavior. The values for $\rho_{\rm c}$, β, γ' are obtained from [14,17]. The values of $\nu_\perp$ are obtained from the scaling relation $\gamma' = \nu_\perp D - 2\beta$ [19].

D	$\rho_{\rm c}$	β	γ'	$\nu_\perp$	$\nu_\parallel$	$\nu_{\rm l}$	$\theta_{\rm g}$	$\theta_{\rm l}$
2	0.34494	0.637	0.384	0.83	1.21	1.10	1.58	1.41
3	0.2179	0.837	0.18	0.62	1.04	1.04	1.54	1.19
4	0.1571	1^*	0^*	1/2	1	1	1.5	1
5	0.1230	1	0	1/2	1	1.075	1.5	1

References

1. B. Derrida, A. J. Bray, and C. Godrèche, J. Phys. A **27**, L357 (1994).
2. A. J. Bray, B. Derrida, and C. Godrèche, Europhys. Lett. **27**, 175 (1994).
3. D. Stauffer, J. Phys. A **27**, 5029 (1994).
4. S. N. Majumdar, A. J. Bray, S. J. Corwell, and C. Sire, Phys. Rev. Lett. **77**, 3704 (1996).
5. S. Cueille and C. Sire, J. Phys. A **30**, L791 (1997).
6. S. N. Majumdar, Curr. Sci. India **77**, 370 (1999).
7. B. Derrida, V. Hakim, and V. Pasquier, Phys. Rev. Lett. **75**, 751 (1995).
8. B. P. Lee and A. D. Rutenberg, Phys. Rev. Lett. **79**, 4842 (1997).
9. K. Oerding and F. van Wijland, J. Phys. A **31**, 7011 (1998).
10. H. Hinrichsen and M. Antoni, Phys. Rev. E **57**, 2650 (1998).
11. E. V. Albano and M. A. Muñoz, Phys. Rev. E **63**, 031104 (2001).
12. R. M. Ziff, E. Gulari, and Y. Barshad, Phys. Rev. Lett. **56**, 2553 (1986).
13. M. Rossi, R. Pastor-Satorras, and A. Vespignani, Phys. Rev. Lett. **85**, 1803 (2000).
14. S. Lübeck, Phys. Rev. E **64**, 016123 (2001).
15. H. Hinrichsen, Adv. Phys. **49**, 815 (2000).
16. H. Hinrichsen and H. M. Koduvely, Eur. Phys. J. B **5**, 257 (1998).
17. S. Lübeck and A. Hucht, J. Phys. A **34**, L577 (2001).
18. G. R. Grimmet and D. R. Stirzaker, *Probability and Random Processes* (Clarendon Press, Oxford, 1992).
19. I. Jensen and R. Dickman, Phys. Rev. E **48**, 1710 (1993).